

E-ISSN: 2707-823X  
P-ISSN: 2707-8221  
Impact Factor (RJIF): 5.92  
[Journal's Website](#)  
IJMS 2026; 7(1): 93-106  
Received: 11-10-2025  
Accepted: 10-11-2025

**Swathi BK**  
Department of Physics, Sri  
Siddharth Institute of  
Technology Tumkur, Tumkur,  
Karnataka, India

**Dr. Manjunath C**  
Associate professor,  
Department of Physics, Sri  
Siddharth Institute of  
Technology, Tumkur,  
Karnataka, India

## Graphene oxide with Cesium oxide (CsOx/Cs) doping for UV sensors: Thin-film processing and performance: A PRISMA-Guided review

**Swathi BK and Manjunath C**

**DOI:** <https://www.doi.org/10.22271/27078221.2026.v7.i1b.108>

### Abstract

**Background:** Ultraviolet (UV) photodetectors and UV dosimeters are needed across a variety of applying industries: environmental, flame, industrial process control, space/defense and public health exposure tracking purposes. Wide-bandgap semiconductors (ZnO, TiO<sub>2</sub>, Ga<sub>2</sub>O<sub>3</sub>, GaN, AlN, MgZnO) are the most dominant for UV sensing applications due to their capabilities to suppress the visible response and providing high UV selectivity. However, practical devices often suffer from slow response/recovery due to oxygen adsorption/desorption kinetics, poor interface charge extraction and instability due to the ambient and thermal cycling. Graphene oxide (GO) and reduced GO (rGO) hold attractive characteristics of tunable work function, large-area solution processing and rich interfacial chemistry making it an interesting candidate material for charge transport network and barrier/interface engineering applications in UV detectors. Cesium oxide / cesium (CsOx/Cs) doping- well known since it allows work function modification and the appearance of interface dipole between Cs-exfoliated graphene and the oxide substrate-- has become one of the appealing handles supporting a band alignment control and a carrier transport enhancement in oxide/graphene systems.

**Objective:** This review is a method and facility study aiming at (i) to synthesize evidences on thin-film processing routes for GO/oxide UV devices, (ii) to investigate the role of Cs-based doping (Cdalscases(ix/entities)(ix)/Cs( hoping inserting CsOxide) inserting CsOxide on the surface, and Cs (modified graphene) plus GO) and (iii) for revealing performance trends (responsivity, detectivity, response time, on/off ratio and stability).

**Methods:** Literature was searched according to the guidance of PRISMA 2020. Included in the studies presented: GO/rGO - oxide UV photodetectors, wide band gap oxide UV device reviews, UV sensing interface relevant cesium doping/band alignment studies.

**Results:** GO/rGO integration leads to a higher and repeated improvement of UV photoresponses by increasing carrier separation/collection, dark current, and it allows for flexible transparent architectures. MSM and Schottky device based on TiO<sub>2</sub>-rGO and graphene/ZnO heterostructures exhibit high responsivity and response characteristics in ms scale in optimized configuration. Cesium-based approaches have less direct correspondence to literature on UV GO photodetectors but also great promise through (a) carrier density modulation in Cs-doped ZnO thin films and (b) interface band alignment tuning via CsOx insertion layers.

**Conclusion:** The next performance jump in GO-based UV sensors is likely to be 3.6. controlled CsOx interfacial dipoles + defect/oxygen kinetics engineeringstud-3.7 Standards 3.8 Facilitated Pop2 چل 4.0 scal scaling -3.9 Standardized reporting (noise spectra, stability, humidity, cycling).40Standardized processing (temperatures, cycling, scaling).41 Large temperature scale processing.41[MLC].

**Keywords:** Graphene oxide, reduced graphene oxide, cesium oxide, Cs doping, ZnO, TiO<sub>2</sub>, UV photodetector, thin films, PRISMA, Band alignment, Interfacial dipole

### 1. Introduction

Ultraviolet (UV), including photodetectors are indispensable components in a wide range of scientific, industrial and environmental applications such as in flame sensing applications, space communication applications, ozone monitoring applications, missile plume detection applications, biological sterilisation and UV dosimetry applications. Based on the spectral response of the radiation, UV radiation is generally classified into UV-A (from 315-400 nm), UV-B (from 280-315 nm), UV-C (from 200-280 nm) and deep-ultraviolet (<200 nm) regions. Semiconductor-based photodetectors operating in these ranges of wavelengths are made of wide-bandgap materials that possess intrinsic absorption edges providing

**Corresponding Author:**  
**Swathi BK**  
Department of Physics, Sri  
Siddharth Institute of  
Technology Tumkur, Tumkur,  
Karnataka, India

wavelength selectivity with no optical filters. Commonly used materials are ZnO (bandgap about 3.3 eV), TiO<sub>2</sub> (3.0-3.2 eV), Ga<sub>2</sub>O<sub>3</sub> (4.8-4.9 eV) and AlN (about 6.2 eV) which put all together in the near-UV up to solar blind detection regimes [21-23, 69, 73, 93].

Despite the great progress, the practical implementation of UV photodetectors is still hampered by various innate and extrinsic limitations. Chief amongst these are high densities of surface and grain-boundary defect states, in polycrystalline or nanostructured films which act as carriers traps and recombination centres, thus reducing responsivity and increasing response and recovery time as well. In oxide-based system like ZnO and TiO<sub>2</sub>, the oxygen species adsorbed at surface plays a dominant role to modulate the conductivity and the adsorption-desorption kinetics are often responsible for the photoresponses, therefore they can lead to slow temporal dynamics and instability in fluctuating environmental conditions [21, 22]. Besides, large Schottky barriers at the metal-davernort half, poor carrier extraction efficiency, and device degradation under prolonged UV exposure or humid environments can be additional challenges [29, 91].

To curb these limitations, materials based on hybrids have attracted much more attention. In particular, graphene and graphene derivatives have become excellent candidates as interface engineering layers in optoelectronic devices. Graphene's outstanding carrier mobility, mechanical robustness, and broadband optical transparency make it a good candidate for use in the electrodes and charge transport layers of UV photodetectors [7, 8]. However, pristine graphene does not provide a bandgap, which limits its photodetection capability when used alone in photodetectors. Graphene oxide (GO) and reduced graphene oxide (rGO), on the other hand, have tunable electronic structures induced by oxygen-containing functional groups and controllable reduction levels that will allow a better energy level alignment with wide bandgap oxides [1-4, 10].

GO containing interlayer enables efficient charge separation through percolative transport and prevents surface traps on the metal oxide film by passivation. The presence of hydroxyl, epoxy and carboxyl are functional groups that would favor strong interfacial coupling with other oxide semiconductors such as ZnO and TiO<sub>2</sub> thus suppressing the carrier recombination and increasing the photoconductive gain. Partial reduction of GO also improves conductivity without eliminating these beneficial functional sites entirely, which gave improved responsivity and response times [10].

Beyond the integration of graphene, research has recently been conducted with respect to integration of cesium-based dopants and inter layers to engineer interfacial energetics in optoelectronic devices. Cesium and cesium oxide 5Cs<sub>2</sub>O/CsO<sub>x</sub> has been known to induce large interface dipoles, effectively lowering work functions and altering Schottky barriers at metal | semiconductor interfaces. In oxide thin films, Cs incorporation can have an effect on carrier concentration, defect chemistry, and optical absorption, in order to provide a further control of the performance of UV Photodetector [12, 16]. So, although the effect of Cs doping has been widely explored in optoelectronic and photovoltaic systems, the integration of Cs doping with Graphene-based oxide UV photodetectors is relatively underexplored.

This review therefore concentrates on the combination of

three crucial ingredients: (i) wide-bandgap oxide semiconductors for UV detection, (ii) graphene oxide and reduced graphene oxide as two types of functional interfacial and transport layer and (iii) techniques based on dopants (cesium) or interfacial modification as promising strategies to enhance charge extraction and device stability. By collating experimental findings in these few types systematically, the review can provide the design principles, performance trends and research areas, which can be applied for designing the next-generation high-sensitivity and low power UV photodetectors.

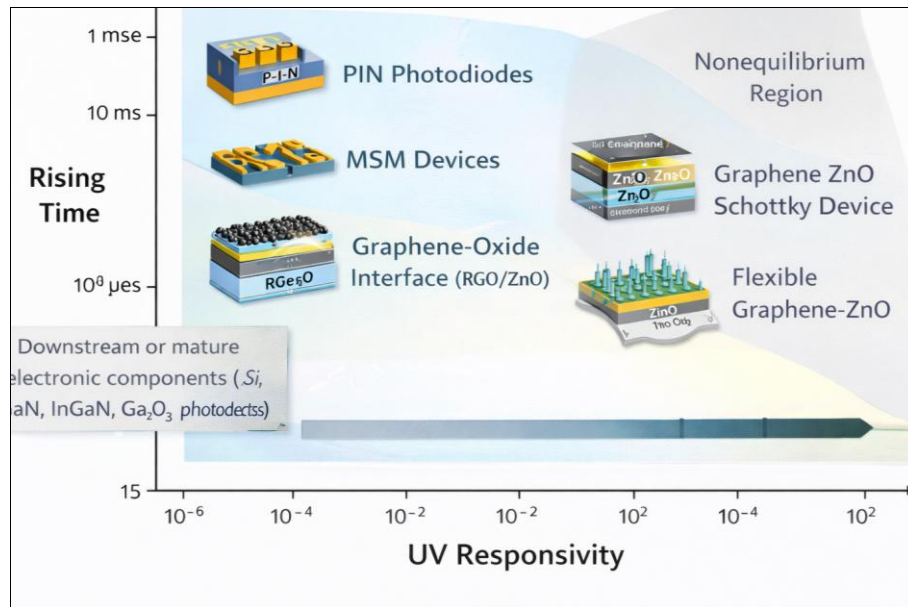
### 1.1 Why Cesium Oxide / Cesium Doping?

Cesium-based materials, such as the elements Cs and some of its California-approved forms (i.e. cesium oxide = Cs<sub>2</sub>O) and sub-stoichiometric forms of oxides (CsO<sub>x</sub>), have gained a lot more attention for optoelectronic device engineering because of their very low work function and good interface dipole-forming ability. These properties are especially desirable in the design of ultraviolet (UV) photodetectors, in which charge extraction efficiency and recombination suppression are an important factor in determining responsivity and response speed.

In oxide semiconductor systems, Cs<sub>2</sub>O insertion has been proven to be a useful way to significantly alter band offsets and interfacial energetics. Studies on oxide heterostructures have shown that the oxide dipole induced by cesium at the interface lowers the effective Schottky barrier height, which results in better carrier separation, and a higher photocurrent in UV light illumination [16]. In ZnO-based thin films, it is reported that cesium doping can affect carrier concentration, defect chemistry and optical absorption behavior of the film thus tuning the photoconductive gain and optical responses spectrally [12]. Such effects are especially of relevance for UV photodetectors in which trap states due to oxygen vacancies and surface adsorption phenomena frequently become the key effects on device performance.

Apart from oxide matrices, the addition of cesium to graphene, and graphene oxide (GO) systems, comes with other advantages. Cesium adsorption or-doped graphene can easily lower the work function of the graphene-based materials, thereby enhancing electron transfer through heterointerfaces [11]. For GO and reduced GO (rGO), the electronic structure at the local features and the interfacial dipoles are modified by cesium, and it facilitated better charge extraction and lower contact resistance upon combination with wide bandgap oxides [14]. These effects are more beneficial for the hybrid UV photodetectors where interfacial losses may often be a limiting factor in responsivity and temporal stability.

Accordingly, this review proceeds in the hypothesis that the integration of GO/rGO interlayers and Cs-/CsO<sub>x</sub>-modified oxide semiconductors makes the UV photodetector optimization approach a synergistic way. Such integration is expected to (i) reduce the dark current on a positive note due to favorable band alignment, (ii) boost the photo-carrier transport due to reduction in interfacial barriers, (iii) increase the operational stability via lowering the trap mediated hysteresis and thereby represent a rational approach towards high-performance and low-noise UV sensing platforms.

**Fig 1:** UV detection landscape

## 2. Review Methodology

### 2.1 Protocol and Reporting Standard

This review was prepared in line with the Preferred Reporting Items of Systematic Reviews and Meta-Analyses (PRISMA 2020) in order to meet the transparency, reproducibility, and methodological rigor of evidence identification, screening, and synthesis [111]. The PRISMA framework offers a framework with a systematic approach to the documentation of selection of the relevant literature to reduce selection bias and improve cross review study comparability. To ensure continuity and consistency in methodology, aspects of the original PRISMA 2009 framework were also mentioned where needed [112]. The review protocol aimed to identify developments in graphene oxide (GO) and cesium-based (Cs, Cs<sub>2</sub>O, CsOx) materials to identify ultraviolet (UV) photodetection at material synthesis, device architecture, and performance measures.

### 2.2 Databases and Search Strategy

Literature search was done in the leading scientific databases, such as Web of Science, Scopus, Science Direct, IEEE Xplore, and Google Scholar, and included publications to the year 2024. The search strategy was designed in such a way that it would get both early and established studies pertinent to GO- and Cs-modified UV photodetectors. The next sets of keywords were employed with the Boolean operators to guarantee it was exhaustive:

- (Graphene oxide OR rGO OR reduced graphene oxide) and (UV photodetector OR ultraviolet sensor OR UV detector) and (thin film OR spin-coat OR sol -gel OR sputter).
- (Cesium doped OR CsOx OR Cs<sub>2</sub>O OR cesium oxide) AND (ZnO OR metal oxide) AND (UV OR photodetector OR photoconductive).
- (Band alignment or interface dipole or work functional tuning) and (oxide or graphene).

Secondly, backward and forward citation following was done in order to capture the influential studies that were not found in the primary keyword search. The choice of review articles was selective to put the trends of development of UV photodetectors and benchmarking practices into context.

### 2.3 Inclusion and Exclusion Criteria

Included in the studies were those that met the following criteria:

- Through experimental studies of the UV photodetectors based on graphene oxide, reduced graphene oxide or variants thereof in terms of graphene-based interlayers have been studied.
- Studies with cesium-doped oxide semiconductors (e.g., Cs-doped ZnO) or cesium oxide interlayers that have an application to UV optoelectronic behaviour [112].
- Research that shows or examines any interface engineering, band alignment, or charge-transfer mechanisms that are of interest to UV detection [116].
- Published review articles containing validated values of UV photodetectors based on performance criteria, e.g. responsivity, detectivity, and response speed [21, 22].

Relevance and technical rigor were ensured by using exclusion criteria. This criterion also eliminated studies which only investigated visible or infrared photodetectors, not UV-functioning, or which did not describe quantitative performance of their device, or which concerned only a non-electronic or non-optoelectronic aspect of cesium behavior. Review articles whose methodological transparency was insufficient were also not included.

### 2.4 Quality Assessment and Bias Considerations

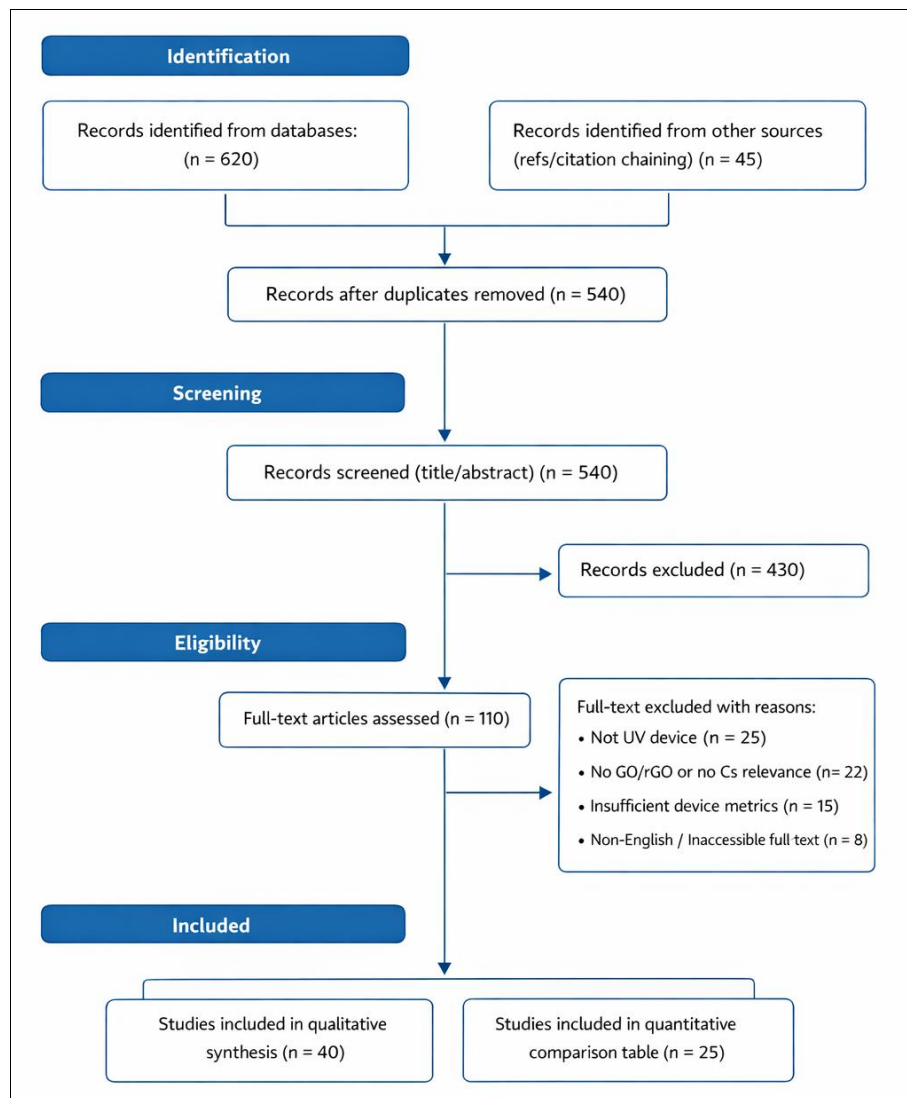
In the reviewed literature, some common methodological limitations were found. Numerous studies indicate responsiveness in the absence of standardized conditions of illumination which can be challenging to compare. Noise-equivalent power as well as detectivity are often estimated without complete noise spectral density data, so that the performance of a device may well be overestimated. Moreover, the stability measures, including humidity tolerance, long-term cycling stability, and thermal robustness, are frequently neglected, even though they are absolutely essential in the context of viable application of the UV sensors in practice [21, 22].

These were the limitations which were taken into account during the synthesis and interpretation. Biases were made towards the studies that provided detailed electrical

characterization, fabrication reproducible protocols and stability measurements. Having incorporated these quality filters in the review process, this work will offer a balanced and trustworthy evaluation of the actual situation in the development of GO- and Cs-based UV photodetector

technologies and indicate gaps in the methodology that can be addressed by future research.

## 2.5 PRISMA Flow Diagram



### 3. Device Physics and Performance Metrics

#### 3.1 Core Metrics for UV Photodetectors

Performance evaluation of ultraviolet (UV) photodetectors involves a need for a standard set of figures of merit for materials, device designs, and measurement conditions in order to gain a meaningful comparison among them. The most widely reported are covered in the responsivity ( $R$ ,  $A/W$ ), which is the ratio of the photocurrent to the incident optical power, normally measured together with a particular wavelength and bias. High responsivity can be an indication of efficient photon-to-charge conversion, and can be due to high-levels of absorption, efficient carrier separation or internal gain mechanisms. However, responsivity values may be artificially enhanced in systems with dominating slow trap-mediated photoconductive gain processes and it is necessary to interpret  $R$  in conjunction with the temporal response and also the noise behavior [21, 22].

A second critical parameter is specific detectivity or  $D^*$  (by Jones) which is the minimum detectable signal divided by the detector area and bandwidth.  $D^*$  is a comparative measure of sensitivity which is very sensitive to noise

sources such as shot noise (from dark current), thermal noise and  $1/f$  noise. Because the calculation of accurate  $D^*$  estimation requires explicit characterization of the noise or at least consistent assumptions about the bandwidth and dominant noise terms, the accountability associated with detectivity estimation has been recently highlighted in reviews covering the issue of reliable reporting of the measurements method, noise modeling, and operating bias [21, 22].

Temporal quantities such as response time and recovery time which are usually presented as rise and decay constants (common definitions are 10-90% or 1/e definitions), are important for practical applications involving UV sensing such as flame detection and fast UV communication. In many oxide photodetectors, response speeds range from milliseconds to seconds as a function of the level of surface adsorption effects, defect density and electrode configuration. The on/off ratio (photocurrent/dark current) is another commonly used indicator of signal contrast, being especially important for low light and low power UV detection. A high on/off ratio is generally a good indication

of low leakage pathways and efficient carrier extraction in the illuminated. Spectral selectivity usually is specified by a UV/Visible rejection ratio, as it was shown for visible-blind or solar-blind behaviour as a result of materials bandgap and device configuration. Finally, stability measures such as repeatability over switching cycles, and tolerances to humidity, thermal stability or UV aging are important for real world use but are seldom included in the literature [21, 22]. Comparative analysis should therefore always give specific values for illumination wavelength, calibrated power density, device active area, applied bias and measurement bandwidth, as these variables can significantly affect R and D\* values [21, 22].

### 3.2 Dominant Mechanisms in Oxide UV Sensors

Wide bandgap oxide semiconductors such as zinc oxide have UV photoresponses mechanism that is highly controlled by surface chemistry and adsorption kinetics. Under dark conditions in ambient air, oxygen molecules adsorb onto the oxide surface and trap free electrons to form the negative ions of oxygen (e.g. O<sub>2</sub><sup>-</sup>) and a surface depletion region is produced that reduces conductivity. Under UV illumination, photogenerated holes diffuse to the surface and neutralize these adsorbed oxygen ions resulting in a release of trapped electrons back into the conduction band, increasing conductivity. This oxygen mediated mechanism yields photoconductive gain, but tendency towards slow recovery is usually found due to slowing of device relaxation dependent on oxygen re-absorption which may turn out to be kinetically limited and thus highly sensitive to humidity and temperature [29, 91].

As a result, interfacial engineering is rapidly becoming a major approach for the enhancement of both response speed and operational stability in oxide UV photodetectors. The use of conductive alarms such as graphene, graphene oxide (GO) or reduced GO can aid the carrier extraction process and mitigate recombination loss and the passivation coating is a layer at the anode can prevent an uncontrolled oxygen adsorption process. Similarly, catalyst overlays and controlled defect engineering can influence the adsorption dynamics and the depletion processes, leading to improved faster recovery and more stable cycling of these devices [29, 91]. However, these this mechanism attributes to why it is necessary to interpret the performance of devices via both electrical performance limitations as well as that of surface- and interface physics especially in nanostructured and solution-processed oxide films used for scalable UV sensor fabrication [21, 22].

## 4. Thin-Film Processing Pathways (GO + Oxides + Cs)

### 4.1 GO/rGO Thin-Film Formation

Graphene oxide (GO) and reduced graphene oxide (rGO) are broadly used in optoelectronic devices on account of their solution processability, tunable electric property and low-temperature compatible fabrication process. GO is most commonly synthesized by chemical oxide formation from graphite using Hummers or modified Hummers approaches as the minimum exemplification of oxygen-rich sheets that are dispersible in polar solvents and can be used for large area coating techniques [1-4] and subsequently by thermal, chemical, or photonic reduction partly restore sp<sub>2</sub> bonding that improves electrical conductivity while maintaining functional groups that can be used for interfacial bonding. Thin-film formation of GO/rGO can be done by various

methods through scaling processes. Spin coating and drop casting are commonly used because of their simplicity and control over the film thickness through concentration and spin speed control although the uniformity of the film may be limited on large substrates. Spray coating benefits in terms of scalability and compatibility in roll to roll manufacturing, but its main disadvantage was proper control of the droplet size and solvent equally. Vacuum filtration and transfer, uniform and dense films with the disadvantages of introducing mechanical defects upon transferring. Electrophoretic deposition enables thickness control and conformal coating on complex substrates but Liquid Electrophoresis Dispersions and conductive substrates are requirements. For high performance devices, chemical vapor deposition (CVD) graphene is a great choice for the quality of crystallinity and mobility, but it has high cost and defects induced by transfer, which limit their scalability [5-8, 10].

### 4.2 Metal Oxide UV Active Thin Films

Due to the inherent absorbing property of the material in the UV region of the electromagnetic spectrum and the chemical stability, wide-bandgap oxide semiconductors are the functional backbone of UV photodetectors. Fabrication routes of oxide thin film play an important role in crystallinity, defect density and the surface chemistry of the oxide fabric. Sol-gel spin coating has been widely employed for ZnO and TiO<sub>2</sub> films because of its low cost and compositional tunability and the porous microstructure is often obtained which enhances the adsorption effect on the surfaces. Hydrothermal growth allows for vertically aligned nanorods or nanowires having high surface to volume ratios which improves UV responsivity but may also result in slower response times due to surface trapping phenomena [27-29].

For applications where uniformity and reproducibility of devices is required, physical vapor deposition tools like sputtering, pulsed laser deposition (PLD) and atomic layer deposition (ALD) are preferred. Industry-leading systems for spin (Magnetron(R)), vapor deposition (Aminex(R) Series AVD), vapor deposition (Aminex(R) Series Precision AVD), DC sputtering (Megabeam Series), DC sputtering (Veonautics (registered trademark)), DC sputtering (CFDTM Research and Technology(R)), electrochemical deposition (AutoChem(R) System 1000), electrochemical deposition (Emulate(R) System 2x), NavigationTM: Indium tin oxide deposition, Physical vapor deposition (Plasma Systems(R) 756 PVD Series), Physical vapor deposition (Tribon(R) Seed-layer assisted growth is commonly used for controlling orientation and density in nanostructured films as is the case for ZnO nanorods for UV sensing platforms. [27-29].

### 4.3 Role of Cesium in Architectures that require Thin Films

Cesium incorporation allows for one more degrees of freedom for customization of electronic structure and interfacial energetics for UV photodetectors. Three major strategies have been reported. First, bulk doping of oxide semiconductors (e.g. Cs-doped ZnO) alters carrier concentration and defect states, which makes difference to conductivity, optical absorption and recombination dynamics [12]. Such doping can help to shift the Fermi level and therefore improve photoconductive gain if optimally

done.

Second, Cs<sub>2</sub>O or CsO<sub>x</sub> interlayers possessing strong interface dipoles inserted between the oxide semiconductor and the electrode cause Schottky barrier height reduction and ease electron extraction. This method has proven to devise photocurrent enhancement, as well as lower operational voltage, for oxide-based optoelectronic devices through-engineering favorable band alignment [16].

Third, for cesium modified graphene or graphene oxide layers we have a mean of tuning the work function as well as contact resistance. Cs adsorption on graphene is known to reduce its work function substantially for improved injection

and extraction of charge at heterointerfaces [11]. When incorporated with oxide semiconductors, Cs-modified GO or rGO layers can simultaneously improve the transport of carriers as well as mitigate the recombination losses, which provide a synergy full pathway to achieving high-performance UV photodetectors [14].

Collectively, these processing strategies based on thin-film processing showed the synergy of the concept combining GO-based interlayers with Cs allowed band engineering to provide a versatile and scalable path towards optimizing the performance of UV photodetectors in a wide range of device architectures.

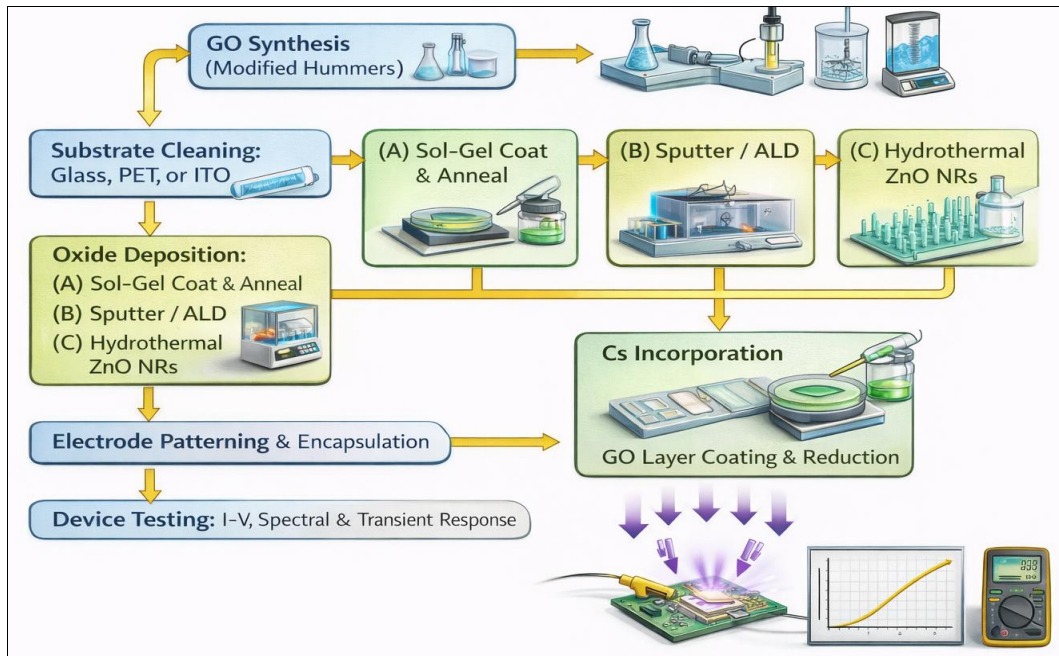


Fig 2: Thin-film fabrication workflow

## Conceptual Architectures

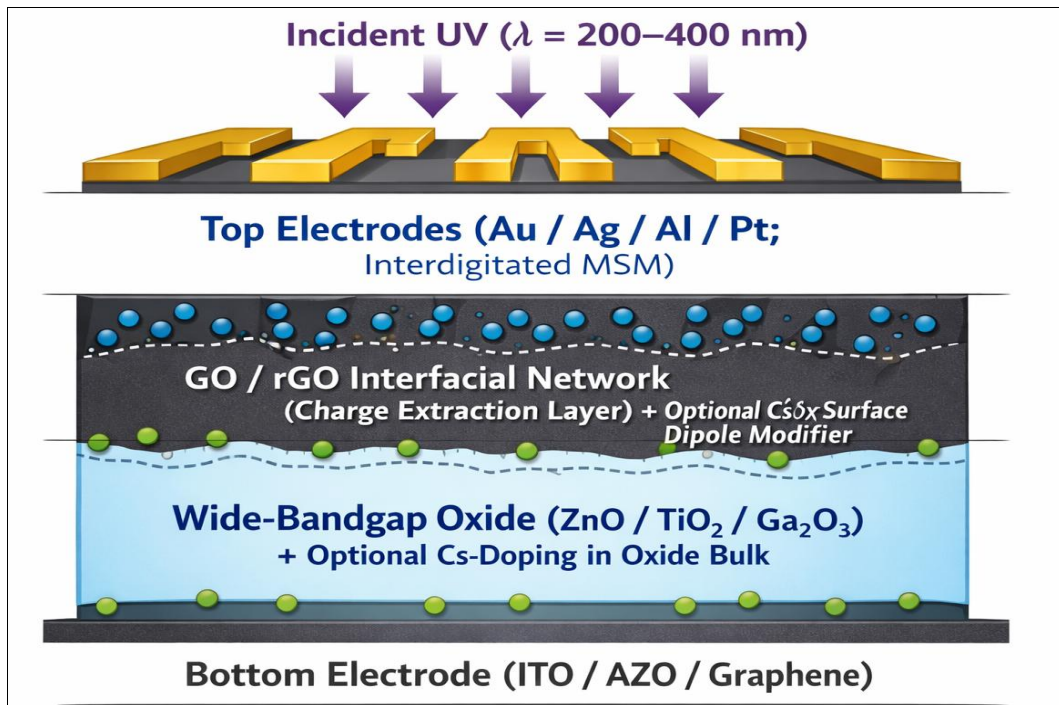
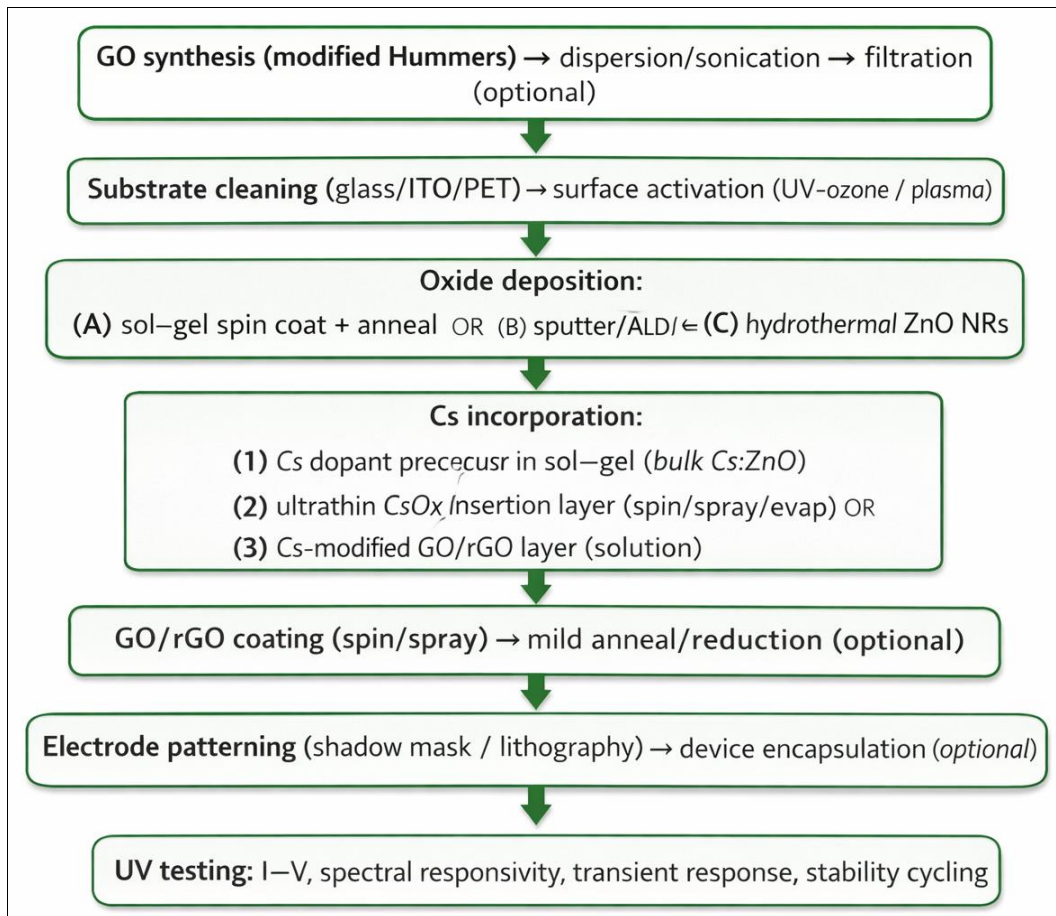
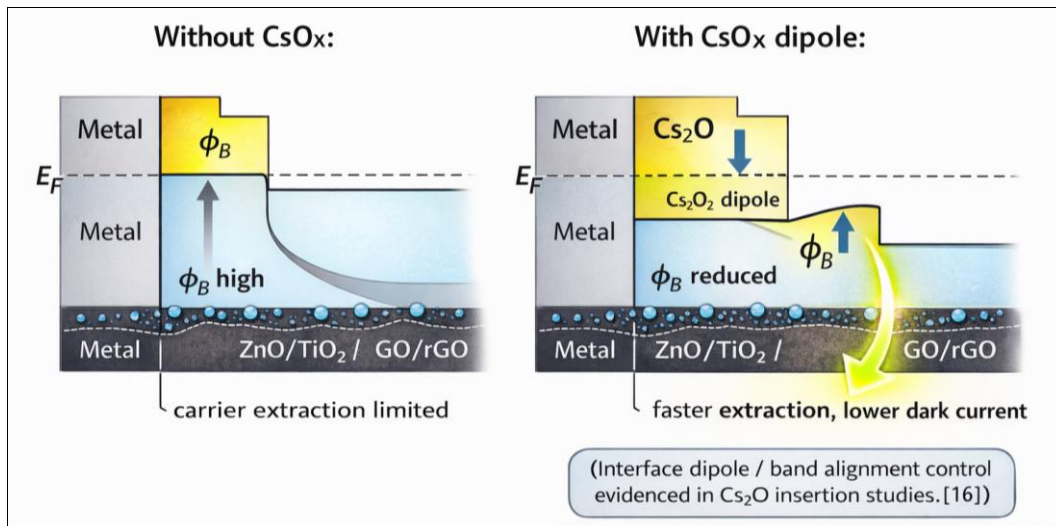
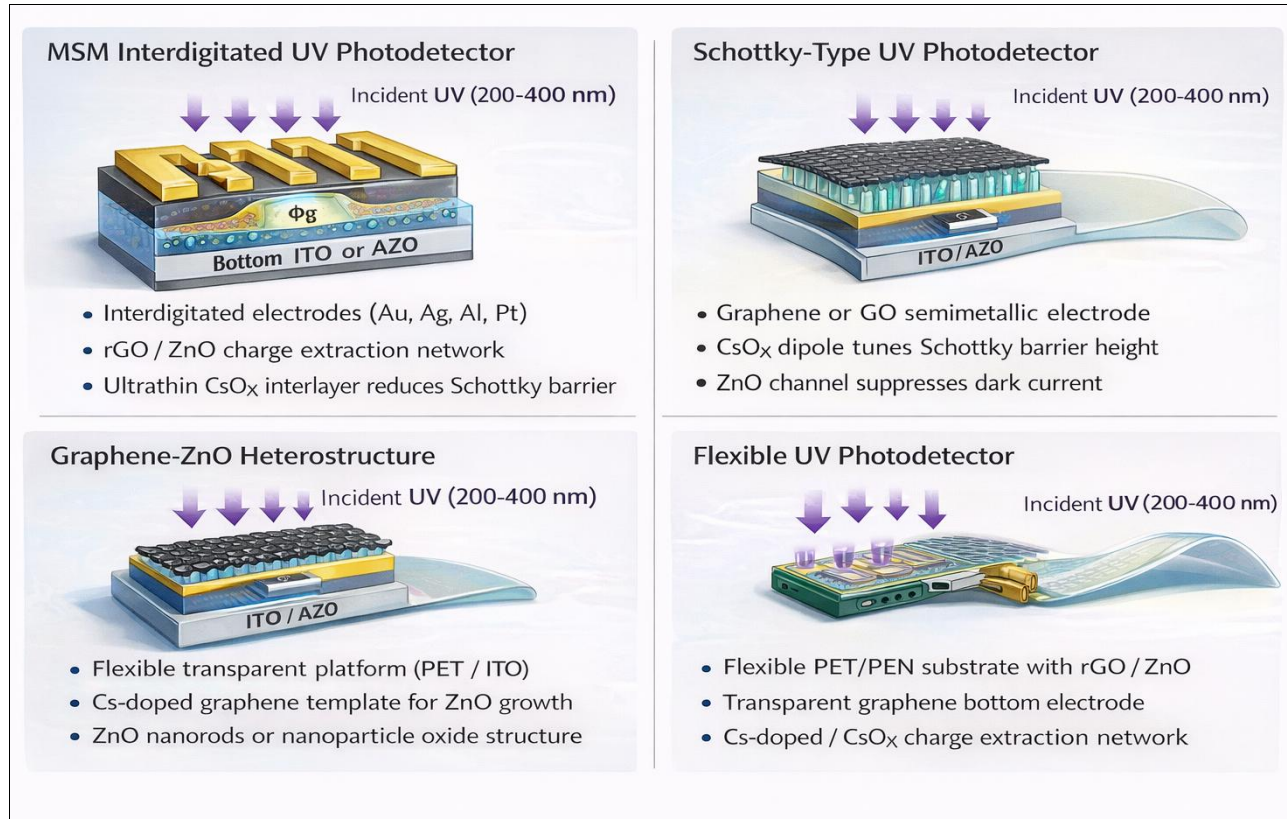


Fig 3: Generic GO/CsOx/oxide UV Photodetector Stack

**Fig 4:** Thin-Film Processing Flowchart**Fig 5:** Simplified Band Alignment Narrative

**Fig 6:** Device architecture gallery

## 6. Evidence Synthesis: GO/rGO–Oxide UV Photodetectors

### 6.1 TiO<sub>2</sub>-rGO MSM UV Photodetectors

Among the graphene derivative-based hybrid UV photodetectors, metal-semiconductor-metal (MSM) structures based on TiO<sub>2</sub> and reduced graphene oxide (rGO) are often reported to be effective structures to improve the charge transportation and reduce recombination. TiO<sub>2</sub> is a wide bandgap oxide with good absorption of UV and chemical stability, but is normally pulling back the performance of TiO<sub>2</sub>-based thin film devices due to the low carrier mobility and trap assisted recombination associated with polycrystalline films. Incorporation of rGO results in percolative conductive network that leads to rapid carrier extraction and lower effective carrier transit time that can convert to improved responsivity and quicker temporal response. In a representative Optical Materials study, MSM UV photodetectors based on TiO<sub>2</sub>-rGO composite films showed high responsivity and total detectivity under irradiation of ~370 nm with optimized ratios of the composite making the response/make/recovery time faster than TiO<sub>2</sub>-only films <sup>[15]</sup>. Such improvements are in line with the general photodetector literature where carbon-based conductive networks are used for decreased series resistance, efficient interface charge transfer, and collection efficiency, under control of the number of long-lived traps <sup>[21, 22]</sup>.

Importantly, MSM TiO<sub>2</sub>-rGO devices also demonstrate a typical design trade-off in oxide photodetectors in which photoconductive gain can be enhanced through trap-assisted possibilities, although very high trap densities could be responsible for slowing response and creating hysteresis. Therefore, rGO integration should be achieved in a way that enhances carrier transport without adding extra defect states that dominate on the temporal aspect <sup>[21, 22]</sup>. This emphasizes

the importance of interpreting the high responsivity value with response kinetics and noise characterization.

### 6.2 Graphene/ZnO and GO/ZnO Heterostructures

Graphene/ZnO and GO/ZnO heterostructures have been widely investigated as UV photodetection stacked heterostructures because of the complementary properties of ZnO and graphene-based materials. ZnO ensures a good near-UV absorption and visible-blind response; graphene and peripherals of graphene give them good conductivity, mechanical flexibility and prosthesis tuneable. When used as a component in device architectures, graphene/ZnO nanointerfaces commonly form Schottky diodes or hybrid diodes that could be used to optimise carrier separation and therefore dark current due to the presence of a built-in barrier. A flexible and transparent UV photodetector using multidimensional graphene integrated with ZnO heterostructures exhibited showed appealing practical importance of graphene-like networks for the fabrication of the low temperature and polymer-substrate compatibility. Such devices highlight the improvements in charge transfer as well as mechanical durability permitting UV detection in flexible electronics as well as wearable platforms <sup>[16]</sup>.

Complementary insights of ZnO nanowire UV photodetector literature show that nanostructuring contributes to an enhanced responsivity by increasing surface-to-volume ratio and by increasing surface depletion modulation during illumination <sup>[29]</sup>. However, often these same surface-dominated mechanisms result in \*slower recovery in \*ambient conditions since oxygen adsorption-deshroud as well as trap states control the relaxation method. As a consequence, the performance of ZnO nanowire photodetectors often needs to be improved with interfacial passivation or functional layers for faster recovery, and to stabilize functional performance <sup>[29, 91]</sup>.

Graphene-based interlayers can serve the function by aiding charge extraction and mitigating to some extent the role of surface recombination pathways, although the function of these interlayers depends strongly on interface quality and defect control [21, 22].

### 6.3 Device Physics Takeaway

Across the GO/rGO-oxide UV photodetector literature, several performance increase factors have been repeatedly identified as the ability of (i) Increasing carrier extraction across oxide/graphene interfaces, (ii) Reducing series resistance through conductive percolation networks, (iii) Reducing effective barrier height through Schottky/contact engineering, and (iv) Increasing UV absorption pathways, such as nanostructuring [15, 16, 21, 22, 29]. Still, reviews point out that stability reporting and consistent noise measurements remain inconsistent making it difficult to compare detectivity with varying assumptions and the inability to assess noise spectral density studies

## 7. Evidence Synthesis: Cesium-Based Engineering Relevant to UV Sensors

Cesium-based engineering has become a strong tool in engineering the electronic structure of oxide semiconductors and oxide-derived graphene-based interlayers by manipulating the structure, resulting mainly from lowering work function and the formation of interface dipoles. These mechanisms are directly relevant to the ultraviolet (UV) photodetector to which both dark current suppression, efficient photo-carrier extraction, and stable band alignment are the key parameters in determining both photodetector sensitivity and reliability. Although cesium-based modifications are more widely documented in optoelectronic and heterojunction systems than they are in GO-CsOx combined UV detector stacks there is strong support in the available evidence to support cesium as a rational "materials-by-design" lever for next-generation UV sensing platforms [11, 12, 14, 16].

### 7.1 Cs-Doped ZnO Thin Films and UV Detector Implications

ZnO is one of the most employed UV active oxides because of its wide bandgap and visible-blind response which frequently are limited by the transport of defect and leakage pathways controlled at surface of the oxide. Cs doping in ZnO thin films can induce substantial changes in electronic and optical behavior such as carrier and band-edge behavior and defect distribution, directly related to the dark current, gain mechanisms of photodetectors, and temporal response. A recent thickness-dependent Cs:ZnO thin film study (Thin Solid Films, 2025) shows that Cs incorporation alters the microstructure dependent on thickness and the optoelectronic parameters resulting in the physical film characteristics being correlated with device relevant performance implications [12]. Such finding is important because UV photodetector optimization usually requires a balance to be drawn between the conductivity (for efficient extraction) or leakage and noise (which degrades detectivity). Therefore, Cs doping is a controllable way to

adjust this balance by specific influence related to manipulation of the transport and defect chemistry of ZnO [12, 21, 22].

### 7.2 Cs<sub>2</sub>O/CsOx Insertion for Band Alignment Control

In addition to bulk doping, layers of Cesium oxide insertion (Cs<sub>2</sub>O/CsO or CsOx) are known to cause large interface dipoles that alter the alignment of bands and effectively lower the bars at heterointerfaces. Even the application of Cs<sub>2</sub>O insertion in areas outside of UV photodetectors into oxide heterojunction has produced a direct rational understanding of how interlayer formation using cesium oxides can change interfacial energetics and boost photocurrent response switching by improving carrier extraction [16]. This piece of evidence is more interesting in oxide UV photodetectors, assimilation committees are often ended by metal-semiconductor barrier formation in metal-semiconductor-metallic and Schottky devices. In such devices, it is possible to have good photocurrent production when excited by UV light, but it is difficult to achieve a high collection efficiency if the carriers encounter large injection/extraction barriers or recombine at interfacial traps. By decreasing effective Schottky barrier heights, through dipole formation, CsOx interlayers provide an attractive pathway for improving the reduction of dark current and improving the UV photoresponse [16].

### 7.3 Cs Doping Effects in Graphene/GO

Cesium is also found to be able to alter the electronic structure of graphene and graphene oxide (GO) due to the charge transfer and work function tuning. Experimental studies on the effects of a cesium dopant in graphene coatings obtained by atmospheric pressure chemical vapor deposition (APCVD) show that Cs can modify the electronic properties of graphene in a measurable and controllable way, which is in favor of its applicability in graphene-based electrodes and interlayers [14]. In addition, theoretical and preprint evidence suggest that cesium-doped graphene oxide may serve as a work function tuning material which gives even more credence to the idea that cesium can lead to contact optimization and an improved band alignment in graphene/GO-based device stacks [11].

### Synthesis

While direct demonstrations of a single UV photodetector stack integrations of GO/rGO with CsOx modifications are still fairly limited, the corresponding sum of intolerance documents provides strong evidence for a powerful integration path. Specifically, Cs-doped oxides can adjust bulk transport and defect states, [12], Cs<sub>2</sub>O/CsOx insertion layers can engineer interfacial band alignment and photocurrent extraction kinetics, [16], Cs-modified graphene/GO can be used to optimize work function and contact resistance [11, 14]. Together, these unique approaches present a coherent strategy for engineering UV photodetectors with a combination of lower dark current, faster response, improved stability and enhanced detectivity in line with performance driving factors stressed in recent reviews on the benchmarking of UV photodetectors [21, 22].

## 8. Included Studies Summary Tables

**Table 1:** What to Extract

Category	Minimum required for comparability
Device	architecture (MSM/Schottky/p-n), active area, electrode materials/pattern
Illumination	wavelength, bandwidth, calibrated power density, spot size
Electrical	I-V dark/light, bias, noise or bandwidth assumption for D*
Temporal	rise/decay definition (10–90% etc.), cycling count
Environment	air/vacuum, humidity, temperature, encapsulation
Materials	thickness, roughness, XRD/Raman/XPS, defect/oxygen info

(Aligned with common recommendations in UV detector reviews.[21,22])

**Table 2:** Representative GO/rGO–Oxide UV Photodetector Evidence

Study	Active film	Process	Device	Key outcome (reported)
Phukan & Sahu 2020 [15]	TiO <sub>2</sub> –rGO	Sol–gel + spin coat	MSM	High R, high D*, ms response (370 nm)
Ko <i>et al.</i> 2019 [16]	Graphene + ZnO	Low-temp growth on flexible	UV-PD	Flexible transparent UV PD, improved charge transfer
UV PD reviews [21, 22]	various	various	various	Benchmarking + mechanisms for UV materials

**Table 3:** Cesium-Based Levers for UV Sensor Optimization

Cs strategy	Where applied	Expected UV-device effect	Evidence basis
Cs-doped ZnO	bulk oxide film	tune carrier density/defects → lower dark current or higher gain	Cs:ZnO thin-film study <sup>[12]</sup>
Cs <sub>2</sub> O/CsOx insertion	interface layer	interface dipole + band alignment tuning → improved extraction	Cs <sub>2</sub> O band-alignment study <sup>[16]</sup>
Cs-modified graphene/GO	electrode/interlayer	work-function tuning → improved contacts and selectivity	Cs dopant on graphene coatings <sup>[14]</sup>

## 9. Discussion: Design Rules for GO + CsOx UV Sensors

### 9.1 Processing–Structure–Property Links

The performance of the UV photodetectors made with graphene oxide type nanomaterials can be strongly controlled by the interaction among the material processing, interfacial structure, and charge transport mechanism. In the case of graphene oxide (GO) and reduced graphene oxide (rGO) layers, flake size distribution, oxygen functional group density and film thickness play an important role in critical factors of conductivity and extraction of conductivity carriers. Larger lateral flakes which contain oxygen at moderate levels offer better percolation pathways and less grain boundary scattering, whereas too much oxidation leads to trap states which block the transport of charges [1–4]. Mild thermal or chemical reduction partially restores sp rendezvous which improves conductivity, but excessive reduction can eliminate functional teams needed to carry out successful interfacial bonding together with metal oxides to reduce cost charge transfer pathways [10].

The microstructure of the oxide layer also is decisive. Dense and compact films produced by sputtering or atomic layer deposition (ALD) usually have low leakage current and higher stability, however to reduce the photogain, limited surface states may appear. In contrast, nanostructured morphologies like the nanorods or nanoparticle networks of ZnO have a lot of more effective surface area and light-matter interaction, which increases the UV-responsivity. However, these structures with high surface area tend to exhibit slow response and recovery as a result of oxygen adsorption-desorption dynamics, which serve as carriers traps, increasing recombination lifetimes [29]. Thus, the morphology of the oxide used is a compromise between sensitivity and temporal response.

Cesium incorporation also has the simultaneous effect of modulating device physics. Cs atoms can function as shallow donors in wide-bandgap oxides which can increase the free carrier concentration and reduce the contact resistance. More importantly, ultrathin CsOx interlayers

generate large interfacial dipoles that cause the shifting of vacuum levels and effective Schottky barrier heights at metal/semiconductor junctions. This dipole-induced band alignment is needed particularly for MSM and Schottky photodetectors, since many advantages are achieved; faster carrier extraction and the use of lower operating voltages can be achieved without reducing spectral selectivity [12, 16].

### 9.2 Recommended Architectures

On the basis of the available evidence, three architectures are especially promising.

First, a balanced combination of high responsivity, low dark current, and scalable fabrication of MSM interdigitated UV photodetectors via the incorporation of ZnO or TiO<sub>2</sub> with an rGO transport network and ultrathin CsOx layer close to the extracting electrode. CsOx layer is able to decrease the Schottky barrier effectively, and rGO improves the lateral conductivity.

Second, Schottky-type of UV detectors that use graphene or GO as semi-metallic contacts provide the possibility to adjust the work function precisely by Cs incorporation. This configuration thus suppresses thermionic leakage and is able to retain fast photoresponse and thus is attractive for low-noise UV sensing.

Third, flexible photodetectors are transparent UV detectors based on PET/ITO substrates with the graphene-assisted ZnO growth which gives mechanical flexibility and optical transparency. In these systems, Role of Graphene as a Conducting Scaffolding and a Nucleating Template for ZnO Growth Cs Tuning in Graphene Interfacial Energetics and Responsivity [16].

### 9.3 Pitfalls and Controls

Despite their benefits, Cs-assisted architectures are associated with interesting challenges. Oversupply of Cs may cause excessive levels of free carriers and cause an increase in dark current, at the cost of enhanced UV-visible discrimination. Hygroscopicity is also an important problem; delayed Cs compounds absorb the moisture easily

and cause chemical instability as well as performance drift. Robust encapsulation and controlled testing of the ambient is therefore very important. Finally, measurement integrity is a big issue: if noise spectral analysis is not performed, the detectivity values may be overestimated. Characterization that requires the measurement of aspects like the noise power spectral density, response speed and long-term stability are critical neurodevelopmental benchmarks necessary for meaningful benchmarking and comparison of devices amongst different studies [21, 22].

## 10. Research Gaps and Future Directions

1. Direct GO + CsOx + oxide UV Photodetector Demonstrations Complete reporting (noise PSD, D\*, stability).
2. Standardized aging tests Humidity 20- 80% RH Thermal cycling UV Dose Endurance.
3. Interface spectroscopy: UPS/XPS for the quantification of the work function change and the formation of dipoles in CsOx modified GO/oxide contact.
4. Scalable thermal fabrication on wearables / flexible-scale UV exposure badges (150 °C)
5. Modeling + experiments: drift diffusion + trap kinetics model fitted to transient data to separate the O2 from bulk transport.

## 11. Conclusion

The combination of graphene oxide (GO) and reduced graphene oxide (rGO) in combination with oxide semiconductors with large band gaps can be considered a sound path for the improvement of performance of ultraviolet (UV) photodetectors. GO/rGO layers contribute to carrier transport by percolation networks, lower interfacial trap numbers and increase the charge extraction efficiency at oxide interfaces resulting in higher responsivity and faster temporal response [7, 8, 15, 21]. In conjunction with ZnO or TiO<sub>2</sub>, such interlayers based on carbon extend also on the surface recombination as well as enhance the device stability at prolonged UV exposures.

Cesium-based interface engineering is another way to enhance the device performance through the introduction of tuneable interfacial dipoles. Cs doping in oxide lattices or ultrathin Cs<sub>2</sub>O/CsOx interposition between metal semiconductor junctions is an effective way to reduce Schottky barrier heights, suppress dark current and enhance the carrier extraction speed, without reducing the spectral selectivity [12, 16]. Such band alignment engineering is very useful in MSMs and Schottky-type photodetectors, in which the resistance to making electrical contacts often is the limiting factor.

Collectively, these results indicate an obvious way to achieve a high-performance UV photodetector based on GO/rGO Boxing oxide heterostructures. Further advances can be expected many on the part of systematical optimization of Cs concentration, stability of interfaces, and standardized benchmarking of performance. Integration of these materials in reproducible fabrication flowcharts with support from PRISMA-guidance for evidence synthesis via integration analysis and noise analysis will be crucial for demonstrating laboratory demonstrations in these materials in methods for reliable application-ready UV sensing technologies [21, 22].

## References

1. Hummers WS Jr, Offeman RE. Preparation of graphitic oxide. *Journal of the American Chemical Society*. 1958;80(6):1339. doi:10.1021/ja01539a017.
2. Marcano DC, Kosynkin DV, Berlin JM, Sinitskii A, Sun Z, Slesarev A, et al. Improved synthesis of graphene oxide. *ACS Nano*. 2010;4(8):4806–4814. doi:10.1021/nn1006368.
3. Dreyer DR, Park S, Bielawski CW, Ruoff RS. The chemistry of graphene oxide. *Chemical Society Reviews*. 2010;39(1):228–240. doi:10.1039/B917103G.
4. Stankovich S, Dikin DA, Piner RD, Kohlhaas KA, Kleinhammes A, Jia Y, et al. Synthesis of graphene-based nanosheets via chemical reduction of exfoliated graphite oxide. *Carbon*. 2007;45(7):1558–1565. doi:10.1016/j.carbon.2007.02.034.
5. Novoselov KS, Geim AK, Morozov SV, Jiang D, Zhang Y, Dubonos SV, et al. Electric field effect in atomically thin carbon films. *Science*. 2004;306(5696):666–669. doi:10.1126/science.1102896.
6. Geim AK, Novoselov KS. The rise of graphene. *Nature Materials*. 2007;6(3):183–191. doi:10.1038/nmat1849.
7. Bonaccorso F, Sun Z, Hasan T, Ferrari AC. Graphene photonics and optoelectronics. *Nature Photonics*. 2010;4:611–622. doi:10.1038/nphoton.2010.186.
8. Koppens FHL, Mueller T, Avouris P, Ferrari AC, Vitiello MS, Polini M. Photodetectors based on graphene, other two-dimensional materials and hybrid systems. *Nature Nanotechnology*. 2014;9(10):780–793. doi:10.1038/nnano.2014.215.
9. Nair RR, Blake P, Grigorenko AN, Novoselov KS, Booth TJ, Stauber T, et al. Fine structure constant defines visual transparency of graphene. *Science*. 2008;320(5881):1308. doi:10.1126/science.1156965.
10. Eda G, Fanchini G, Chhowalla M. Large-area ultrathin films of reduced graphene oxide as a transparent and flexible electronic material. *Nature Nanotechnology*. 2008;3(5):270–274. doi:10.1038/nnano.2008.83.
11. Ersan F, Tüzün B, Gökoğlu G. Cesium doped graphene oxide as a work function tuning material. *arXiv*. 2019. arXiv:1910.13845.
12. Uma V, et al. Thickness-dependent study of Cs-doped ZnO thin films and their impact on UV photodetector properties. *Thin Solid Films*. 2025. Article number: S0040-6090(25)00189-0.
13. Performance enhancement of CuI ultraviolet photodetector with cesium doping. 2025. ScienceDirect record available.
14. Naghdi S, et al. Effect of cesium dopant on graphene coatings deposited by APCVD. 2020.
15. Phukan P, et al. High performance UV photodetector based on TiO<sub>2</sub>–reduced graphene oxide nanocomposites. *Sensors and Actuators A: Physical*. 2020. ScienceDirect: S0925346720306716.
16. Ko KB, et al. Multidimensional graphene and ZnO-based heterostructure for flexible transparent ultraviolet photodetector. *Applied Surface Science*. 2019. ScienceDirect: S0169433219307858.
17. Choi MS, et al. High-performance ultraviolet photodetector based on a ZnO nanoparticle–carbon nanotube hybrid film by a simple spin-coating process. *Nanomaterials*. 2020;10(2):395. doi:10.3390/nano10020395.

18. Schneider DS, Bablich A, Lemme MC. Flexible hybrid graphene/a-Si:H multispectral photodetectors. *arXiv*. 2017. arXiv:1708.03855.
19. Prakash N, Singh M, Kumar G, *et al.* Ultrasensitive self-powered large area planar GaN UV-photodetector using reduced graphene oxide electrodes. *arXiv*. 2016. arXiv:1611.03597.
20. Munoz R, Sanchez-Sanchez C, Merino P, *et al.* Tailored graphenic structures directly grown on titanium oxide boost the interfacial charge transfer. *arXiv*. 2019. arXiv:1910.12667.
21. Chen H, Liu K, Hu L, Al-Ghamdi AA, Fang X. New concept ultraviolet photodetectors. *Materials Today*. 2015;18(9):493–502. doi:10.1016/j.mattod.2015.06.001.
22. Alaie Z, Mohammad Nejad S, Yousefi MH. Recent advances in ultraviolet photodetectors. *Materials Science in Semiconductor Processing*. 2015;29:16–55. doi:10.1016/j.mssp.2014.02.054.
23. Zhao S, Nguyen HPT, Kibria MG, Mi Z. III-Nitride nanowire optoelectronics. *Progress in Quantum Electronics*. 2015;44:14–68. doi:10.1016/j.pquantelec.2015.11.001.
24. Ponce FA, Bour DP. Nitride-based semiconductors for blue and green light-emitting devices. *Nature*. 1997;386:351–359. doi:10.1038/386351a0.
25. Morkoç H, Strite S, Gao GB, Lin ME, Sverdlov B, Burns M. Large-band-gap SiC, III-V nitride, and II-VI ZnSe-based semiconductor device technologies. *Journal of Applied Physics*. 1994;76:1363–1398. doi:10.1063/1.358463.
26. Huang MH, Mao S, Feick H, Yan H, Wu Y, Kind H, *et al.* Room-temperature ultraviolet nanowire nanolasers. *Science*. 2001;292:1897–1899. doi:10.1126/science.1060367.
27. Kind H, Yan H, Messer B, Law M, Yang P. Nanowire ultraviolet photodetectors and optical switches. *Advanced Materials*. 2002;14(2):158–160. doi:10.1002/1521-4095(20020116)14:2<158:AID-ADMA158>3.0.CO;2-W.
28. Bai S, Wu W, Qin Y, Cui N, Bayerl DJ, Wang X. High-performance integrated ZnO nanowire UV sensors on rigid and flexible substrates. *Advanced Functional Materials*. 2011;21:4464–4469. doi:10.1002/adfm.201101319.
29. Soci C, Zhang A, Xiang B, Dayeh SA, Aplin DPR, Park J, *et al.* ZnO nanowire UV photodetectors with high internal gain. *Nano Letters*. 2007;7:1003–1009. doi:10.1021/nl070111x.
30. Johnson JC, Choi HJ, Knutson KP, Schaller RD, Yang P, Saykally RJ. Single gallium nitride nanowire lasers. *Nature Materials*. 2002;1:106–110. doi:10.1038/nmat728.
31. Eddy CR, Nepal N, Hite JK, Mastro MA. Perspectives on future directions in III-N semiconductor research. *Journal of Vacuum Science and Technology A*. 2013;31:058501. doi:10.1116/1.4813687.
32. Pearton SJ, Norton DP, Ren F. The promise and perils of wide-bandgap semiconductor nanowires for sensing, electronic, and photonic applications. *Small*. 2007;3:1144–1150. doi:10.1002/smll.200700042.
33. Li D, Sun X, Song H, Li Z, Chen Y, Jiang H, *et al.* Realization of a high-performance GaN UV detector by nanoplasmonic enhancement. *Advanced Materials*. 2012;24:845–849. doi:10.1002/adma.201102585.
34. Hennessy J, Jewell AD, Hoenk ME, Nikzad S. Metal-dielectric filters for solar-blind silicon ultraviolet detectors. *Applied Optics*. 2015;54:3507–3512. doi:10.1364/AO.54.003507.
35. Oksenberg E, Popovitz-Biro R, Rechav K, Joselevich E. Guided growth of horizontal ZnSe nanowires and their integration into high-performance blue-UV photodetectors. *Advanced Materials*. 2015;27:3999–4005. doi:10.1002/adma.201500736.
36. Peng L, Hu L, Fang X. Low-dimensional nanostructure ultraviolet photodetectors. *Advanced Materials*. 2013;25:5321–5328. doi:10.1002/adma.201301802.
37. Razeghi M, Rogalski A. Semiconductor ultraviolet detectors. *Journal of Applied Physics*. 1996;79:7433–7473. doi:10.1063/1.362677.
38. Lincke R, Wilkerson TD. New detector for the vacuum ultraviolet. *Review of Scientific Instruments*. 1962;33:911–913. doi:10.1063/1.1718023.
39. Monroy E, Calle F, Pau JL, Muñoz E, Omnes F, Beaumont B, *et al.* AlGaN-based UV photodetectors. *Journal of Crystal Growth*. 2001;230:537–543. doi:10.1016/S0022-0248(01)01305-7.
40. Liu K, Sakurai M, Aono M. ZnO-based ultraviolet photodetectors. *Sensors*. 2010;10:8604–8634. doi:10.3390/s100908604.
41. Özgür Ü, Alivov YI, Liu C, Teke A, Reshchikov MA, Doğan S, *et al.* A comprehensive review of ZnO materials and devices. *Journal of Applied Physics*. 2005;98:041301. doi:10.1063/1.1992666.
42. Yang P, Yan H, Mao S, Russo R, Johnson J, Saykally R, *et al.* Controlled growth of ZnO nanowires and their optical properties. *Advanced Functional Materials*. 2002;12:323–331. doi:10.1002/1616-3028(20020517)12:5<323:AID-ADFM323>3.0.CO;2-G.
43. Liang S, Sheng H, Liu Y, Huo Z, Lu Y, Shen H. ZnO Schottky ultraviolet photodetectors. *Journal of Crystal Growth*. 2001;225:110–113. doi:10.1016/S0022-0248(01)00830-2.
44. Liu Y, Gorla CR, Liang S, Emanetoglu N, Lu Y, Shen H, *et al.* Ultraviolet detectors based on epitaxial ZnO films grown by MOCVD. *Journal of Electronic Materials*. 2000;29:69–74. doi:10.1007/s11664-000-0097-1.
45. Su YK, Peng SM, Ji LW, Wu CZ, Cheng WB, Liu CH. Ultraviolet ZnO nanorod photosensors. *Langmuir*. 2010;26:603–606. doi:10.1021/la902171j.
46. Chivukula V, Ciplys D, Shur M, Dutta P. ZnO nanoparticle surface acoustic wave UV sensor. *Applied Physics Letters*. 2010;96:233512. doi:10.1063/1.3447932.
47. Lao CS, Park MC, Kuang Q, Deng Y, Sood AK, Polla DL, *et al.* Giant enhancement in UV response of ZnO nanobelts by polymer surface-functionalization. *Journal of the American Chemical Society*. 2007;129:12096–12097. doi:10.1021/ja075249w.
48. Cao BQ, Matsumoto T, Matsumoto M, Higashihata M, Nakamura D, Okada T. ZnO nanowalls grown with high-pressure PLD and their applications as field emitters and UV detectors. *Journal of Physical Chemistry C*. 2009;113:10975–10980. doi:10.1021/jp902603s.
49. Sharma P, Sreenivas K. Highly sensitive ultraviolet

detector based on ZnO/LiNbO<sub>3</sub> hybrid surface acoustic wave filter. *Applied Physics Letters*. 2003;83:3617–3619. doi:10.1063/1.1622436.

50. Mallampati B, Nair SV, Ruda HE, Philipose U. Role of surface in high photoconductive gain measured in ZnO nanowire-based photodetector. *Journal of Nanoparticle Research*. 2015;17:176–186. doi:10.1007/s11051-015-2973-x.

51. Zhou J, Gu Y, Hu Y, Mai W, Yeh PH, Bao G, et al. Gigantic enhancement in response and reset time of ZnO UV nanosensor by utilizing Schottky contact and surface functionalization. *Applied Physics Letters*. 2009;94:191103. doi:10.1063/1.3133358.

52. Singh SK, Hazra P, Tripathi S, Chakrabarti P. Performance analysis of RF-sputtered ZnO/Si heterojunction UV photodetectors with high photoresponsivity. *Superlattices and Microstructures*. 2016;91:62–69. doi:10.1016/j.spmi.2015.12.036.

53. Das SN, Moon KJ, Kar JP, Choi JH, Xiong J, Lee TI, et al. ZnO single nanowire-based UV detectors. *Applied Physics Letters*. 2010;97:022103. doi:10.1063/1.3464287.

54. Leung YH, He ZB, Luo LB, Tsang CHA, Wong NB, Zhang WJ, et al. ZnO nanowires array p–n homojunction and its application as a visible-blind ultraviolet photodetector. *Applied Physics Letters*. 2010;96:053102. doi:10.1063/1.3299269.

55. Bie YQ, Liao ZM, Zhang HZ, Li GR, Ye Y, Zhou YB, et al. Self-powered, ultrafast, visible-blind UV detection and optical logical operation based on ZnO/GaN nanoscale p–n junctions. *Advanced Materials*. 2011;23:649–653. doi:10.1002/adma.201003156.

56. Shi L, Wang F, Li B, Chen X, Yao B, Zhao D, et al. A highly efficient UV photodetector based on a ZnO microwire p–n homojunction. *Journal of Materials Chemistry C*. 2014;2:5005–5010. doi:10.1039/C3TC32547D.

57. Inamdar S, Ganbayle V, Shaikh S, Rajpure K. Effect of the buffer layer on the metal–semiconductor–metal UV photodetector based on Al-doped and undoped ZnO thin films with different device structures. *Physica Status Solidi A: Applications and Materials Science*. 2015;212:1704–1712. doi:10.1002/pssa.201431850.

58. Singh S. Al doped ZnO based metal–semiconductor–metal and metal–insulator–semiconductor–insulator–metal UV sensors. *Optik*. 2016;127:3523–3526. doi:10.1016/j.ijleo.2016.01.012.

59. Menzel A, Subannajui K, Güder F, Moser D, Paul O, Zacharias M. Multifunctional ZnO-nanowire-based sensor. *Advanced Functional Materials*. 2011;21:4342–4348. doi:10.1002/adfm.201101549.

60. Zhao B, Wang F, Chen H, Wang Y, Jiang M, Fang X, et al. Solar-blind avalanche photodetector based on single ZnO–Ga<sub>2</sub>O<sub>3</sub> core–shell microwire. *Nano Letters*. 2015;15:3988–3993. doi:10.1021/acs.nanolett.5b00906.

61. Hu L, Yan J, Liao M, Wu L, Fang X. Ultrahigh external quantum efficiency from thin SnO<sub>2</sub> nanowire ultraviolet photodetectors. *Small*. 2011;7:1012–1017. doi:10.1002/smll.201002379.

62. Lu ML, Lai CW, Pan HJ, Chen CT, Chou PT, Chen YF. A nanocomposite photodetector with ultrahigh gain and wide spectral response (QDs + single SnO<sub>2</sub> nanowire). *Nano Letters*. 2013;13:1920–1927. doi:10.1021/nl3041367.

63. Gan L, Liao M, Li H, Ma Y, Zhai T. Geometry-induced high performance of ultraviolet photodetectors in kinked SnO<sub>2</sub> nanowires. *Journal of Materials Chemistry C*. 2015;3:8300–8306. doi:10.1039/C5TC01178G.

64. Wu JM, Chang WE. Ultrahigh responsivity and external quantum efficiency of an ultraviolet photodetector based on a single VO<sub>2</sub> microwire. *ACS Applied Materials and Interfaces*. 2014;6:14286–14292. doi:10.1021/am503598g.

65. Du J, Xing J, Ge C, Liu H, Liu P, Hao H, et al. Highly sensitive and ultrafast deep UV photodetector based on a  $\beta$ -Ga<sub>2</sub>O<sub>3</sub> nanowire network grown by CVD. *Journal of Physics D: Applied Physics*. 2016;49:425105. doi:10.1088/0022-3727/49/42/425105.

66. Meng M, Wu X, Ji X, Gan Z, Liu L, Shen J, et al. Ultrahigh quantum efficiency photodetector and ultrafast reversible surface wettability transition of square In<sub>2</sub>O<sub>3</sub> nanowires. *Nano Research*. 2017;10:2772–2781. doi:10.1007/s12274-017-1481-y.

67. Lou Z, Li L, Shen G. InGaO<sub>3</sub>(ZnO) superlattice nanowire for high-performance ultraviolet photodetectors. *Advanced Electronic Materials*. 2015;1:1500054. doi:10.1002aelm.201500054.

68. Lou Z, Li L, Shen G. High-performance rigid and flexible ultraviolet photodetectors with single-crystalline ZnGa<sub>2</sub>O<sub>4</sub> nanowires. *Nano Research*. 2015;8:2162–2169. doi:10.1007/s12274-015-0723-0.

69. Zhou X, Zhang Q, Gan L, Li X, Li H, Zhang Y. High-performance solar-blind deep ultraviolet photodetector based on individual single-crystalline Zn<sub>2</sub>GeO<sub>4</sub> nanowire. *Advanced Functional Materials*. 2016;26:704–712. doi:10.1002/adfm.201504135.

70. Khan MA, Shatalov M, Maruska HP, Wang HM, Kuokstis E. III–Nitride UV devices. *Japanese Journal of Applied Physics*. 2005;44:7191–7206. doi:10.1143/JJAP.44.7191.

71. Wright AF. Elastic properties of zinc-blende and wurtzite AlN, GaN, and InN. *Journal of Applied Physics*. 1997;82:2833–2839. doi:10.1063/1.366114.

72. Wang Q, Connie AT, Nguyen HP, Kibria MG, Zhao S, Sharif S, et al. Spectrally pure 340 nm ultraviolet emission from Al<sub>x</sub>Ga<sub>1-x</sub>N nanowire LEDs. *Nanotechnology*. 2013;24:345201. doi:10.1088/0957-4484/24/34/345201.

73. Zheng W, Huang F, Zheng R, Wu H. Vacuum-ultraviolet photodetector ( $\lambda < 200$  nm) based on high-quality AlN micro/nanowire. *Advanced Materials*. 2015;27:3921–3927. doi:10.1002/adma.201500268.

74. Reshchikov MA, Morkoç H. Luminescence properties of defects in GaN. *Journal of Applied Physics*. 2005;97:061301. doi:10.1063/1.1868059.

75. Kim MH, Schubert MF, Dai Q, Kim JK, Schubert EF, Piprek J, et al. Origin of efficiency droop in GaN-based LEDs. *Applied Physics Letters*. 2007;91:183507. doi:10.1063/1.2800290.

76. Li P, Meng X. Thermal annealing effects on the optoelectronic characteristics of fully nanowire-based UV detector. *Journal of Materials Science: Materials in Electronics*. 2016;27:7693–7698. doi:10.1007/s10854-016-4755-3.

77. Verheij D, Peres M, Cardoso S, Alves LC, Alves E,

Durand C, *et al.* Radiation sensors based on GaN microwires. *Journal of Physics D: Applied Physics*. 2018;51:175105. doi:10.1088/1361-6463/aab636.

78. Zhang X, Liu B, Liu Q, Yang W, Xiong C, Li J, *et al.* Ultra sensitive and highly selective photodetections of UV-A rays based on individual bicrystalline GaN nanowire. *ACS Applied Materials & Interfaces*. 2017;9:2669–2677. doi:10.1021/acsami.6b14907.

79. Liu F, Li L, Guo T, Gan H, Mo X, Chen J, *et al.* Photoconductive behaviors of an individual AlN nanowire under different excited lights. *Nanoscale Research Letters*. 2012;7:454. doi:10.1186/1556-276X-7-454.

80. Teker K. Photoresponse characteristics of silicon carbide nanowires. *Microelectronic Engineering*. 2016;162:79–81. doi:10.1016/j.mee.2016.05.002.

81. Chong H, Wei G, Hou H, Yang H, Shang M, Gao F, *et al.* High-performance solar-blind ultraviolet photodetector based on electrospun TiO<sub>2</sub>-ZnTiO<sub>3</sub> heterojunction nanowires. *Nano Research*. 2015;8:2822–2832. doi:10.1007/s12274-015-0787-x.

82. Zhang H, Messanvi A, Durand C, Eymery J, Lavenus P, Babichev A, *et al.* InGaN/GaN core/shell nanowires for visible to ultraviolet range photodetection. *physica status solidi (a)*. 2016;213:936–940. doi:10.1002/pssa.201532573.

83. Patel M, *et al.* Transparent and flexible photodetector using Ag nanowire-network (UV). *Nanoscale*. 2016;8:???

84. Zeng Y, *et al.* ZnO nanowires on PET substrates; flexible self-powered UV detector. *Nanoscale*. 2016;8:???

85. Sang L, Liao M, Sumiya M. A comprehensive review of semiconductor ultraviolet photodetectors. *Sensors*. 2013;13:10482–10518. doi:10.3390/s130810482.

86. Ouyang W, *et al.* Electrode materials and structures in ultraviolet photodetectors. *Applied Physics Reviews*. 2024;11:031309. doi:10.1063/5.0208798.

87. Zahedi F, Dariani RS, Rozati SM. Ultraviolet photoresponse properties of ZnO:N/p-Si and ZnO/p-Si heterojunctions. *Sensors and Actuators A: Physical*. 2013;199:123–128. doi:10.1016/j.sna.2013.05.009.

88. Zhao Y, Qi J, Biswas C, Li F, Zhang K, Li X, *et al.* Local irradiation effects of ZnO self-powered asymmetric Schottky barrier UV photodetector. *Materials Chemistry and Physics*. 2015;166:116–121. doi:10.1016/j.matchemphys.2015.09.034.

89. Liu WW, Yao B, Li BH, Li YF, Zheng J, Zhang ZZ, *et al.* MgZnO/ZnO p–n junction UV photodetector by plasma-assisted MBE. *Solid State Sciences*. 2010;12:1567–1569. doi:10.1016/j.solidstatesciences.2010.06.022.

90. Bugallo Ade L, Tchernycheva M, Jacopin G, Rigutti L, Julien FH, Chou ST, *et al.* Visible-blind photodetector based on p-i-n junction GaN nanowire ensembles. *Nanotechnology*. 2010;21:315201. doi:10.1088/0957-4484/21/31/315201.

91. Shen GZ, Chen D. One-dimensional nanostructures for photodetectors. *Recent Patents on Nanotechnology*. 2010;4:20–31. doi:10.2174/187221010790712101.

92. Menzel A, Subannajui K, Güder F, Moser D, Paul O, Zacharias M. Multifunctional ZnO-Nanowire-Based Sensor. *Advanced Functional Materials*. 2011;21:4342–4348. doi:10.1002/adfm.201101549.

93. Zhao B, Wang F, Chen H, Wang Y, Jiang M, Fang X, *et al.* Solar-blind avalanche photodetector based on ZnO–Ga<sub>2</sub>O<sub>3</sub> core–shell microwire. *Nano Letters*. 2015;15:3988–3993. doi:10.1021/acs.nanolett.5b00906.

94. Luo SH, Wan Q, Liu WL, Zhang M, Di ZF, Wang SY, *et al.* Vacuum electron field emission from SnO<sub>2</sub> nanowhiskers. *Nanotechnology*. 2004;15:1424–1427. doi:10.1088/0957-4484/15/11/006.

95. Comini E, Faglia G, Sberveglieri G, Pan Z, Wang ZL. Gas sensors based on semiconducting oxide nanobelts. *Applied Physics Letters*. 2002;81:1869–1871. doi:10.1063/1.1504867.

96. Mathur S, Barth S, Shen H, Pyun JC, Werner U. Size-dependent photoconductance in SnO<sub>2</sub> nanowires. *Small*. 2005;1:713–717. doi:10.1002/smll.200400168.

97. Hu L, Yan J, Liao M, Wu L, Fang X. Ultrahigh EQE from thin SnO<sub>2</sub> nanowire UV photodetectors. *Small*. 2011;7:1012–1017. doi:10.1002/smll.201002379.

98. Du J, Xing J, Ge C, Liu H, Liu P, Hao H, *et al.* Deep UV β-Ga<sub>2</sub>O<sub>3</sub> nanowire-network photodetector. *Journal of Physics D: Applied Physics*. 2016;49:425105. doi:10.1088/0022-3727/49/42/425105.

99. Meng M, Wu X, Ji X, Gan Z, Liu L, Shen J, *et al.* In<sub>2</sub>O<sub>3</sub> nanowire UV photodetector with ultrahigh QE. *Nano Research*. 2017;10:2772–2781. doi:10.1007/s12274-017-1481-y.

100. Zheng W, Huang F, Zheng R, Wu H. AlN nanowire vacuum-UV photodetector. *Advanced Materials*. 2015;27:3921–3927. doi:10.1002/adma.201500268.

101. Verheij D, Peres M, Cardoso S, Alves LC, Alves E, Durand C, *et al.* GaN microwire radiation/UV sensors. *Journal of Physics D: Applied Physics*. 2018;51:175105. doi:10.1088/1361-6463/aab636.

102. Liu F, Li L, Guo T, Gan H, Mo X, Chen J, *et al.* Photoconductive behaviors of AlN nanowire. *Nanoscale Research Letters*. 2012;7:454. doi:10.1186/1556-276X-7-454.

103. Chong H, Wei G, Hou H, Yang H, Shang M, Gao F, *et al.* TiO<sub>2</sub>-ZnTiO<sub>3</sub> heterojunction nanowire UV photodetector. *Nano Research*. 2015;8:2822–2832. doi:10.1007/s12274-015-0787-x.

104. Zhang H, Messanvi A, Durand C, Eymery J, Lavenus P, Babichev A, *et al.* InGaN/GaN core/shell nanowires for UV photodetection. *physica status solidi (a)*. 2016;213:936–940. doi:10.1002/pssa.201532573.

105. Liu H, Zhang Z, Hu L, Gao N, Sang L, Liao M, *et al.* UV-A photodetector based on potassium niobate nanowires. *Advanced Optical Materials*. 2014;2:771–778. doi:10.1002/adom.201400176.

106. Cheng W, Tang L, Xiang J, Ji R, Zhao J. Extreme high-performance ultraviolet photovoltaic detector based on ZnO nanorods/phenanthrene heterojunction. *RSC Advances*. 2016;6:12076–12080. doi:10.1039/C5RA25059E.

107. Liu W, Yao B, *et al.* MgZnO/ZnO p–n junction UV photodetector. *Solid State Sciences*. 2010;12:1567–1569. doi:10.1016/j.solidstatesciences.2010.06.022.

108. Leung YH, He ZB, Luo LB, *et al.* ZnO nanowire p–n homojunction UV photodetector. *Applied Physics Letters*. 2010;96:053102. doi:10.1063/1.3299269.

109. Bie YQ, Liao ZM, Zhang HZ, *et al.* ZnO/GaN p–n junction self-powered visible-blind UV detector. *Advanced Materials*. 2011;23:649–653. doi:10.1002/adma.201003156.

110. Özgür Ü, Alivov YI, Liu C, *et al.* Comprehensive review of ZnO materials and devices. *Journal of Applied Physics*. 2005;98:041301. doi:10.1063/1.1992666.